JETIR.ORG ISSN: 2349-5162 | ESTD Year : 2014 | Monthly Issue
JOURNAL OF EMERGING TECHNOLOGIES AND INNOVATIVE RESEARCH (JETIR)
An International Scholarly Open Access, Peer-reviewed, Refereed Journal

EFFICIENT ELIMINATION OF ORGANIC CONTAMINANTS UTILIZING A NANOADSORBENT DERIVED FROM *MORINGA OLEIFERA*

[1]Bhanupriya Mordhiya, [2]Pooja Meena, [3]Rekha Sharma [4]Chetan Selwal

[1]Assistant Professor, [2]Research Scholar, [3]Research Scholar, [4]Assistant Professor
[1,2,3]Department of Chemistry, University of Rajasthan, Jaipur
[4]Govt. Women Engineering College, Jaipur

Abstract: The research paper focuses on preparing a nanoadsorbent derived from *Moringa oleifera* seed pods. This nanoadsorbent was modified using orthophosphoric acid (H_3PO_4) and used as an adsorbent for removing Methylene blue (MB) dye from aqueous solutions. Characterization of the AC-MO (Activated carbon of *Moringa oleifera*) nanoadsorbent was conducted using Scanning Electron Microscopy (SEM), Fourier Transform Infrared Spectroscopy (FTIR), and X-ray Diffraction (XRD) techniques to analyze its structure and properties. In the batch process, various operational parameters such as contact time, initial dye concentration, adsorbent dosage, and pH were studied to determine their impact on the adsorption process. The results indicated that the highest adsorption of methylene blue occurred at pH 7, reaching equilibrium within 90 minutes at an initial MB concentration of 100 mg/L, with an adsorbent dosage of 20 mg/50 mL for each sample. The removal efficiency of MB dye increased with higher pH levels, and pH 7 exhibited the maximum removal capacity for all samples. The adsorption data were analyzed using Langmuir and Freundlich isotherm models, with the Langmuir isotherm model showing the best fit, suggesting maximum monolayer adsorption. Moreover, the pseudo-second-order kinetic model provided the best correlation for the experimental data. Overall, the AC-MO nanoadsorbent proved an effective adsorbent for removing MB dye from aqueous solutions, demonstrating its potential application in water treatment and environmental remediation processes.

Keywords: Nanoadsorbent, *Moringa oleifera*, Methylene blue, Freundlich isotherm, and Langmuir isotherm.

I. INTRODUCTION

The main culprits behind water pollution are extensive industrialization and urbanization, leading to the widespread discharge of wastewater. One particularly concerning issue is the release of dyes, which not only endangers terrestrial life but also poses a high risk to aquatic ecosystems [1,2]. The diverse range of dyes employed in industries like pulp, textile, clothing, fabrics, food, and pharmaceutical cosmetics can give rise to significant issues, as they hinder sunlight penetration into the water and cause harm to aquatic life [3,4]. The most prevalent dye is methylene blue (MB) [5]. Methylene blue, classified as a cationic dye, finds wide application in the textile industry for dyeing cotton, coloring papers, silk, wool, and coating paper and leather. Despite its utility, methylene blue poses potential hazards upon exposure. It can cause eye burns, leading to permanent damage in both humans and aquatic animals. Ingestion of the dye may result in increased diarrhoea, vomiting, gastrointestinal irritation, accelerated heartbeat, and symptoms of mental confusion, shock, and nausea. Moreover, direct contact with methylene blue can irritate the skin [6,7]. Different techniques have been developed to remove dyes from wastewater, such as biodegradation, advanced oxidation, ozonation, and membrane technology [8]. While various techniques are available for dye removal from wastewater, they often come with limitations, such as long processing times and high costs. However, among these methods, adsorption has emerged as a favorable option [9]. Adsorption has shown significant advantages, not only at the laboratory level but also in commercial applications, especially when utilizing readily available biomass precursors like seaweeds and agricultural wastes [10,11]. Its effectiveness, coupled with accessible and renewable resources, makes adsorption a promising approach for tackling dye removal challenges in wastewater treatment.[12] The advantages of adsorption over other methods emphasize its low cost, high effectiveness, reduction of chemical and biological sludge, recyclability of the adsorbent, and the absence of the need for expensive or additional synthesis requirements. [13,14,15] The unique characteristics of nanoadsorbents, such as their high selectivity and adsorption capacity, make them effective in dye removal. Additionally, imaging techniques like SEM and XRD are valuable tools for studying and evaluating their effectiveness.[16].

The primary aim of the research discussed is to synthesize an eco-friendly and cost-effective nanoadsorbent using seed pods of *Moringa oleifera* plant and apply it to remove methylene blue (MB) dye from wastewater. *Moringa oleifera*, commonly called the drumstick tree, is a deciduous shrub that grows rapidly and belongs to the Moringaceae family [17]. It is widely distributed globally, although its origins lie in India. In various regions, this tree is recognized for its drought-resistant nature and serves multiple purposes as a vegetable, medicinal plant, and a source of vegetable oil. Recently, its water-purifying properties have been gaining attention, and numerous studies have explored the potential of using its seed pods for treating water [18, 19]. Additionally, nanoadsorbents derived from *Moringa oleifera* have been successfully employed in removing dyes. Researchers have developed the capabilities to transform what was previously deemed as waste into a valuable and environmentally friendly material suitable for various

applications. One of these applications involves the removal of contaminants, such as dyes, from wastewater, promoting sustainable and eco-friendly practices.

II. MATERIAL AND METHODS

a. Sample collection and pre-treatment

Moringa seed pods were gathered from the Rajasthan University campus in Jaipur, then thoroughly washed with distilled water. Next, they were dried in an oven at 80°C for 6 hours. After the drying process, the seed pods were ground into a powder using a mortar and pestle. Finally, the resulting powder was stored in a vacuum desiccator to maintain its dryness and preserve its properties.

b. Preparation of nanoadsorbent

A precisely weighed 25 g of the prepared adsorbent was placed in a beaker containing 40 ml of ortho-phosphoric acid (H_3PO_4). The content in the beaker was thoroughly mixed and heated until it formed a paste. The resulting paste was then transferred to an evaporating dish and placed in a furnace, where it was heated to 250°C for 40 minutes. Afterward, the material was allowed to cool, and it was washed with distilled water to maintain a pH of 7. Subsequently, the material was oven-dried at 100 °C for 6 hours. It was then ground into a powder using a mortar and pestle and sieved to obtain fine powdered AC-MO nanoadsorbent. This nanoadsorbent was carefully stored in an air-tight container for use in various experiments.

c. Adsorbate used

All chemicals utilized were of analytical grade to ensure the accuracy and reliability of the results. Methylene blue (MB) dye was employed as the adsorbate to assess the adsorption performance of the prepared AC-MO nanoadsorbent. The properties of MB dye are as follows: C.I Number: 52015, C.I Name: Basic blue 9, λ_{max}: 664 nm, Molecular formula: $C_{16}H_{18}ClN_3S$, Molar mass: 319.852 g/mol [20, 21]. Fig.1 displays the chemical structure of MB dye, providing a visual representation of its molecular arrangement.

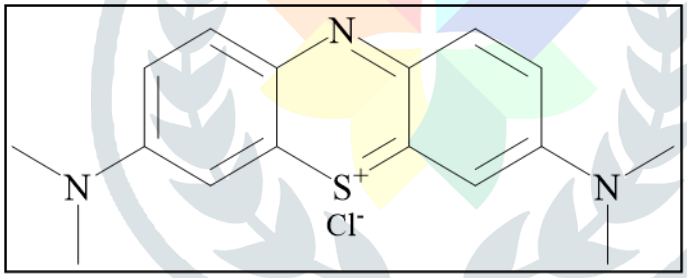

Fig. 1: Structure of Methylene blue (MB) dye

d. Preparation of dye Solution

To prepare a 1000 mg/L dye solution, 1.0 g of MB dye powder was dissolved in 1000 ml of distilled water. This resulted in a solution with a concentration of 1000 mg/L. Subsequently, different dilutions were made by serial dilution using distilled water to obtain various concentrations ranging from 100 to 250 mg/L. Each dilution involved taking a specific volume of the 1000 mg/L dye solution and adding an appropriate volume of distilled water to achieve the desired lower concentrations.

e. Instrumentation

i. Ultraviolet-Visible (UV-Vis) spectrophotometer

The residual concentration of MB dye was measured and analyzed using the Shimadzu UV-2600 Ultraviolet-Visible (UV-Vis) spectrophotometer. This instrument is equipped with 1 cm quartz cells, and the measurement was conducted at a wavelength of 664 nm. The UV-Vis spectrophotometer is a powerful tool commonly used to analyze light absorption by chemical compounds in the ultraviolet and visible regions of the electromagnetic spectrum [22]. In this study, the spectrophotometer was utilized to determine the remaining concentration of MB dye in the solution after adsorption onto the AC-MO nanoadsorbent. By measuring the absorbance of light at a specific wavelength, researchers could quantify the residual concentration of MB dye, which helps evaluate the efficiency of the adsorption process. The UV-Vis spectrophotometer provides accurate and reliable data, enabling researchers to monitor the effectiveness of the nanoadsorbent in removing MB dye from aqueous solutions.

ii. Scanning electron microscopy (SEM)

Scanning Electron Microscopy (SEM) is a powerful technique used to study the surface morphology and characteristics of materials. It operates on the principles of electron-material interactions, where an electron beam is directed at the sample's surface. As a result, certain particles are emitted from the sample, and various detectors analyze these particles to generate a three-dimensional image of the surface [23]. In this study, SEM was employed to investigate the morphological features and surface characteristics of the prepared adsorbents. The Carl Zeiss Evo 18 scanning electron microscope, manufactured in Germany by Carl Zeiss, was used for this purpose. SEM allows for high-resolution imaging, providing detailed information about the adsorbent's surface features, particle size, and shape. By utilizing SEM, researchers can gain a comprehensive understanding of the structure and texture of the adsorbent material, facilitating valuable insights into its properties and potential applications in adsorption processes.

iii. Fourier transform infrared (FTIR)

Fourier Transform Infrared (FTIR) spectroscopy is a valuable analytical technique used to study the surface chemistry of materials by detecting various functional groups and bonding types present in the sample [24]. In this study, the FTIR spectrum was obtained using a Fourier transform infrared spectrometer, specifically the Perkin Elmer FTIR, which operates in the transmittance mode within the spectral range of 4000 to 400 cm^{-1}. The FTIR analysis was conducted on the AC-MO nanoadsorbent to explore the characteristics of functional groups on its surface. This data is crucial for understanding the adsorption mechanisms and interactions between the nanoadsorbent and the target pollutants, enhancing the knowledge of the nanoadsorbent's surface chemistry and its potential effectiveness in water treatment applications.

iv. X-ray Diffraction (XRD)

The crystallinity, phase purity, and particle size of the prepared AC-MO nanoadsorbent were analyzed using X-ray diffraction (XRD) patterns. The XRD pattern was obtained using an X-ray diffractometer [25], specifically the PANalytical X'Pert PRO diffractometer.

The XRD investigates the crystallographic structure and characteristics of the nanoadsorbent by analyzing the XRD pattern; researchers can determine the crystallinity, phase purity, and size of the particles in the nanoadsorbent. This data is crucial for understanding the material's structural properties and assessing its suitability for various applications, particularly in adsorption processes and environmental remediation.

f. Methylene blue adsorption experiment

The adsorption of MB dye on AC-MO nanoadsorbent was conducted using a batch method at room temperature. The study investigated the effects of initial dye concentration, contact time, adsorbent dosage, and pH on the adsorption process. Four initial dye concentrations were used: 100, 150, 200, and 250 mg/L. The experimental procedure involved weighing 0.1 g of adsorbent in a 200 mL Erlenmeyer flask. Then, 100 mL of the MB dye solution was added to the flask. The flask was placed on a magnetic stirrer and shaken at 150 rpm for a predetermined time interval. Sample solutions were withdrawn at specific time points to measure the percentage removal of MB dye from the solution. To determine the residual concentrations of the dye solutions, the absorbance was measured at a wavelength of 664 nm using a UV-Visible spectrophotometer. Equilibrium adsorption capacity (q_e), percentage of dye removal, and adsorption capacity (q_t) were calculated using the following equations (1)-(3):

$$q_e = \left(\frac{C_o - C_e}{m}\right) xV \qquad (1)$$

$$\text{Percentage removal} = \left(\frac{C_o - C_e}{C_o}\right) xV \qquad (2)$$

$$q_t = \left(\frac{C_o - C_e}{m}\right) xV \qquad (3)$$

In the equations (1) to (3) provided in the previous response, C_o represents the initial concentration of MB dye (mg/L), and C_e represents the equilibrium concentration of MB dye (mg/L). V is the volume of the MB dye solution in litters (L), and m is the mass of the adsorbent used in grams (g) [26].

III. Results and Discussions

a. Structural characterization of the prepared nanoadsorbent

The prepared AC-MO nanoadsorbent has been characterized using the following methods

i. Scanning electron microscopy (SEM)

The morphological studies of the AC-MO nanoadsorbent were conducted using SEM analysis. The SEM images, presented in Fig. 2(i-iv) at different magnifications, reveal the surface characteristics of the prepared nanoadsorbent. The micrographs demonstrate that the AC-MO nanoadsorbent possesses a rough surface with irregular channels, which are favorable for dye adsorption and other pollutants. The FESEM micrographs further emphasize the porous morphology of the nanoadsorbent. This porosity is a key feature that makes the AC-MO nanoadsorbent an appropriate material for removing various pollutants from water samples. Overall, the SEM analysis indicates that the nanoadsorbent derived from *Moringa oleifera* exhibits a particle surface that creates a highly porous material. This porous structure enhances the adsorption capability of the nanoadsorbent, making it a promising option for water treatment applications, particularly in the removal of pollutants from aqueous solutions.

ii. Fourier transform infrared (FTIR)

Nanoadsorbent obtained from *Moringa oliefera* contains a significant amount of phosphorus due to the involvement of phosphoric acid in the process. FTIR spectra of AC-MO nanoadsorbent (Fig.3) show multiple functionalities that can also be observed in other carbons acquired by involving phosphoric acid activation of lignocellulosic precursor. The peak at 3813 cm^{-1} and 3451 cm^{-1} are credited to the O-H free stretching [27]. and the peaks at 2885 cm^{-1} and 1776 cm^{-1} indicate the presence of the carboxylic group [28]. The band presence at 2300-2500 cm^{-1} indicates the presence of O=C=O group [29]. The peak at 1776 cm^{-1} indicates the presence of an acid halide group [30]. The peak at 1634 cm^{-1} indicates C=C stretching and the peak at 975 cm^{-1} indicates C=C bending. [31]. The band presence at 1300-1550 cm^{-1} indicates NO_2 group [32].

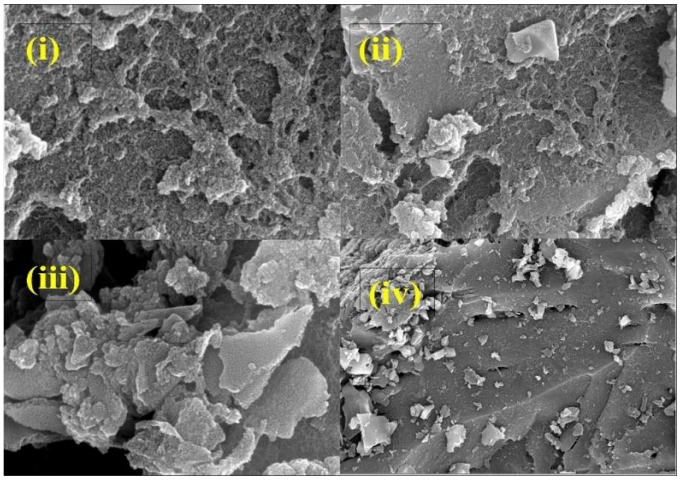

Fig. 2 (i-iv): FESEM images of AC-MO nanoadsorbent

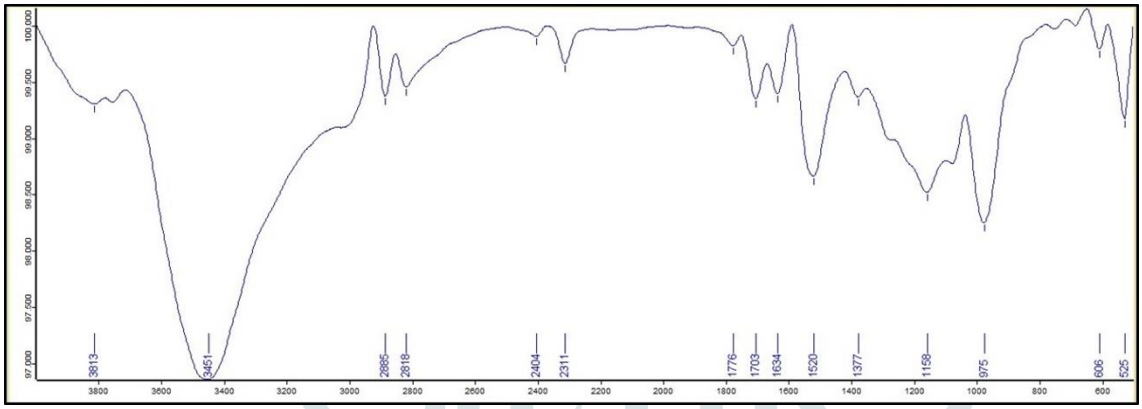

Fig. 3: FTIR spectra of the AC-MO nanoadsorbent

iii. X-ray Diffraction (XRD)

For the AC-MO sample, XRD analysis was carried out several times. XRD patterns of AC-MO nanoadsorbent represented in Fig. 4 reveal that AC-MO nanoadsorbent is amorphous in nature. This material is amorphous but has a hump on the baseline. The elementary chemical composition of samples could explain this characteristic. These results confirm the fact that the activated carbon obtained from agricultural wastes is, for the majority of the time amorphous because of the existence of probable surface functions from which the crystallization is difficult.

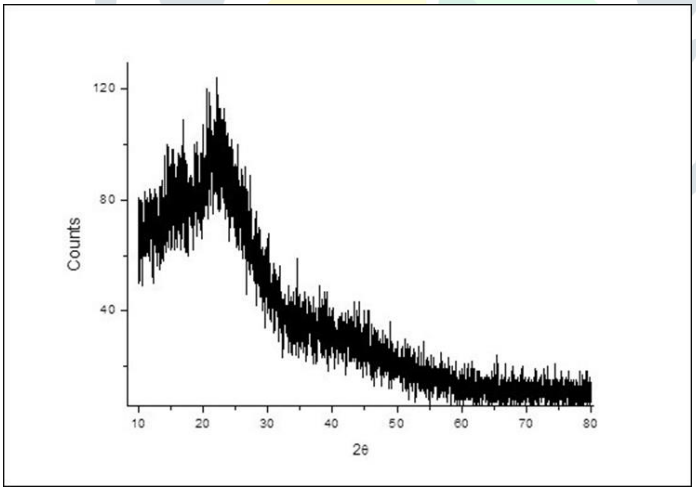

Fig. 4: XRD pattern of the AC-MO nanoadsorbent

b. Batch adsorption studies

i. Effect of contact time

The graphical representation in Fig. 5 demonstrates the influence of different contact times on the percentage removal of methylene blue dye by the AC-MO nanoadsorbent. The data indicates that the amount of MB dye adsorbed increases initially with time but eventually reaches equilibrium at a specific time interval. As shown in Fig. 5, the removal of the dye (adsorbate) exhibits an upward trend with increasing contact time, suggesting that more dye molecules are being adsorbed onto the nanoadsorbent. However, after approximately 90 minutes, the adsorption process reaches a point of equilibrium, where the amount of dye adsorbed remains constant. Based on the graphical representation, it can be concluded that the effective contact time or the time required to achieve equilibrium in the adsorption process is 90 minutes. Beyond this point, further increase in contact time does not significantly affect the percentage removal of methylene blue dye by the AC-MO nanoadsorbent. thus, the effective contact time (equilibrium time) is 90 minutes.

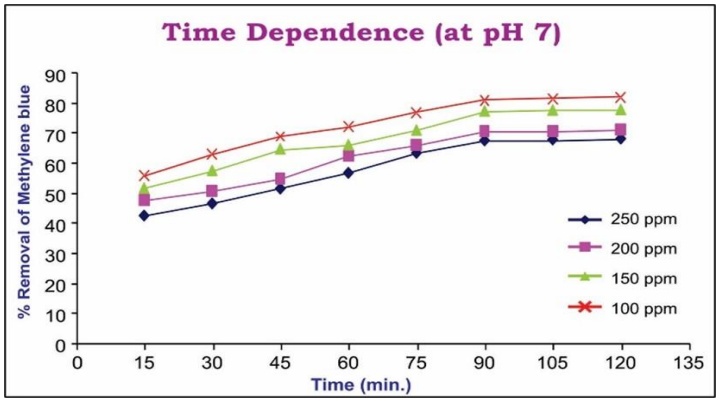

Fig. 5: Effect of contact time on MB adsorption onto AC-MO nanoadsorbent

ii. Effect of initial MB dye concentration

Fig. 6 shows the effect of varying initial MB dye concentrations at the optimum pH of 7 on the percentage removal by the AC-MO nanoadsorbent. The results demonstrate that at a lower initial dye concentration, the removal efficiency is notably higher, reaching 89.3% for the AC-MO nanoadsorbent. However, as the initial dye concentration increases, the adsorption efficiency gradually decreases. This phenomenon can be attributed to the increased number of dye molecules competing for the limited available binding sites on the nanoadsorbent. In summary, the findings suggest that the AC-MO nanoadsorbent exhibits higher efficiency in removing MB dye at lower initial dye concentrations. This is because, at lower concentrations, there are sufficient active sites on the nanoadsorbent surface to accommodate the dye molecules. However, at higher dye concentrations, the available active sites become insufficient to adsorb all the dye species, leading to a decrease in removal efficiency.

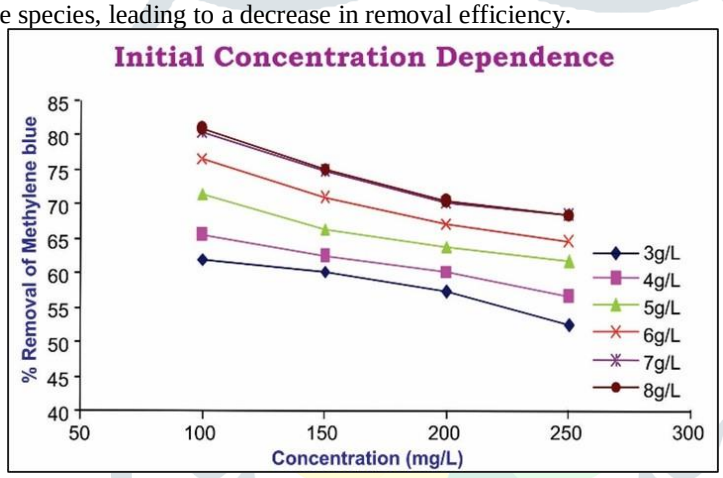

Fig. 6: Effect of initial dye concentration on removal by AC-MO nanoadsorbent

iii. Effect of adsorbent dosage

Fig.7 demonstrates the effect of varying the dose of AC-MO nanoadsorbent on the percentage removal of methylene blue dye. The graph shows that as the dose of AC-MO nanoadsorbent increases, the removal of methylene blue dye also increases, and this trend continues up to a dose of 7 g/L. However, after reaching this dose, the increase in removal becomes relatively small, indicating that the adsorption process becomes less efficient at higher doses. The effective dose of AC-MO nanoadsorbent, where maximum removal efficiency is achieved, is determined to be 7 g/L at pH 7. The reason behind this behavior lies in the greater availability of exchangeable sites or surface area at higher doses of the adsorbent. With an increased dose, more active sites on the AC-MO nanoadsorbent become available for the adsorption of dye molecules, leading to more significant removal of the dye from the solution. As the dose increases beyond the effective dose of 7 g/L, the availability of active sites may become saturated, resulting in a diminished increase in removal efficiency. Therefore, to achieve optimal dye removal, an appropriate dose of 7 g/L is recommended for the AC-MO nanoadsorbent at pH 7.

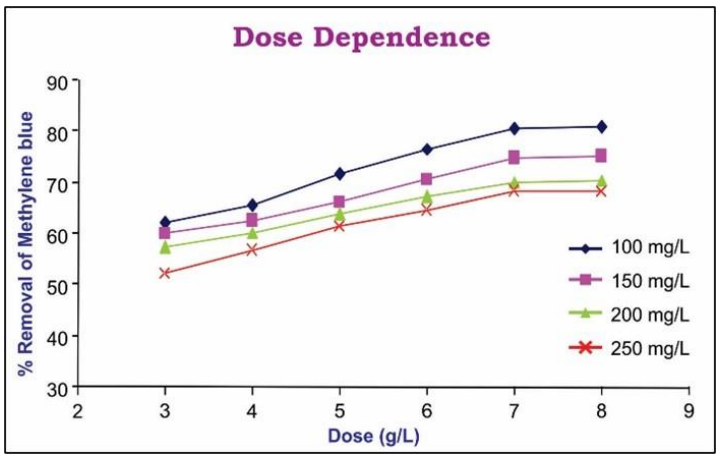

Fig. 7: Effect of adsorbent dose of AC-MO nanoadsorbent for MB dye removal

iv. Effect of pH on dye adsorption

Fig. 8 illustrates the impact of varying the pH values of the dye solution in the range of 5-9 on the adsorption of MB over the AC-MO nanoadsorbent. The graph shows the effect of pH variation on the percentage removal of MB dye by the nanoadsorbent. At low pH values (acidic conditions), the adsorption percentage of MB dye is relatively small. As the pH value increases to 7, the percentage of MB dye removal sharply increases. However, as the pH continues to increase beyond 7, the percentage of dye removal starts to decrease. The observed trend can be explained as follows: At lower pH values in an acidic medium, there is a repulsion between the positively charged surface of the nanoadsorbent and the cationic dye molecules (MB dye). This repulsion reduces the adsorption capacity of the nanoadsorbent for MB dye at lower pH values, leading to lower adsorption percentages. On the other hand, at higher pH values (alkaline conditions), the nanoadsorbent's surface becomes more negatively charged, facilitating the attraction between the negatively charged surface and the cationic dye molecules (MB dye). This increased attraction enhances the adsorption capacity of the nanoadsorbent, resulting in higher adsorption percentages at higher pH values. As a result, the optimum

pH for the adsorption of MB dye onto the AC-MO nanoadsorbent is pH 7, where the percentage removal of MB dye is highest. Beyond this pH, the adsorption efficiency decreases due to the repulsion between the nanoadsorbent's surface and the dye molecules.

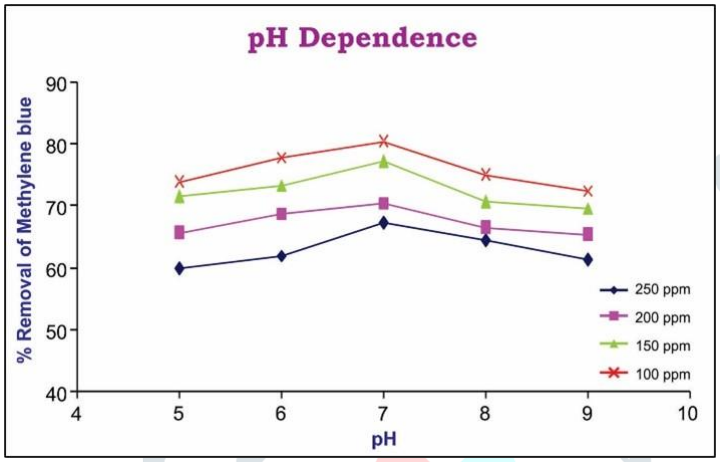

Fig. 8: Effect of pH on MB dye removal by AC-MO nanoadsorbent

c. Adsorption isotherms

In this study, the correlation between the amount of adsorbate (MB dye) adsorbed onto the AC-MO nanoadsorbent and the unabsorbed quantity found in the solution at adsorption equilibrium was investigated using two adsorption isotherm models: the Langmuir and Freundlich models. The Langmuir isotherm assumes that the adsorption occurs on homogeneous surfaces in a monolayer, where all adsorption sites are equivalent and possess equal energy, with no interactions between the adsorbed molecules. On the other hand, the Freundlich isotherm suggests that the adsorption occurs in multilayers on heterogeneous surfaces, with interactions between the adsorbate particles. The Langmuir isotherm equation (Eq. 4) was used to fit the experimental data.

Langmuir isotherm

$$\frac{C_e}{q_e} = \frac{1}{q_{max}\, b_L} + \frac{C_e}{q_{max}} \qquad (4)$$

Where, C_e is the concentration of the adsorbate in solution at equilibrium, q_e is the amount of adsorbate adsorbed, and q_{max} is the maximum adsorption capacity of the adsorbent [33]. The separation factor (R_L) of the Langmuir isotherm (Eq. 5)

$$R_L = \frac{1}{1 + b_L C_o} \qquad (5)$$

indicates the favourability of the adsorption process. R_L values greater than 1 indicate unfavourable adsorption, R_L equal to 1 indicates linear adsorption, R_L values between 0 and 1 indicate favorable adsorption, and R_L equal to 0 indicates irreversible adsorption [34].

The Freundlich isotherm equation (Eq. 6)

Freundlich isotherm

$$\log q_e = \log K_F + \frac{1}{n} \log C_e \qquad (6)$$

involves the Freundlich constants, KF and n, which determine adsorption capacity and adsorption intensity [35], respectively. Both the Langmuir and Freundlich isotherm plots were generated for the adsorption of MB dye onto the AC-MO nanoadsorbent, as shown in Fig. 9 and 10 respectively. Based on the analysis of the isotherm plots and R^2 values, the Langmuir isotherm was found to be more appropriate for describing the adsorption of MB dye onto the AC-MO nanoadsorbent. The R^2 value for the Langmuir isotherm (R2=0.999) was closer to unity, indicating a good fit of the data to the model. This suggests that the adsorption of MB dye occurred in a monolayer on the homogeneous surface of the AC-MO nanoadsorbent.

The value of q_{max} calculated from the Langmuir isotherm model was 71.48 mg/g, indicating the maximum adsorption capacity of the nanoadsorbent for MB dye. The values of R_L (0.3565) and R^2 (0.999) obtained from the Langmuir isotherm plots, suggest that the adsorption of MB dye onto the AC-MO nanoadsorbent is favorable. Overall, the Langmuir isotherm model was the most suitable in describing the adsorption behavior, indicating monolayer adsorption of MB dye on the homogeneous surface of the AC-MO nanoadsorbent. The findings provide valuable insights into the adsorption mechanism and the performance of the nanoadsorbent in removing MB dye from wastewater.

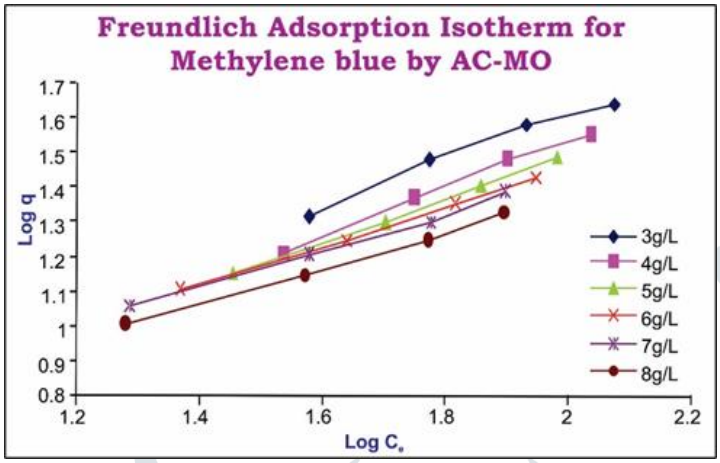

Fig. 9: Freundlich isotherm plot for MB dye adsorption by AC-MO nanoadsorbent.

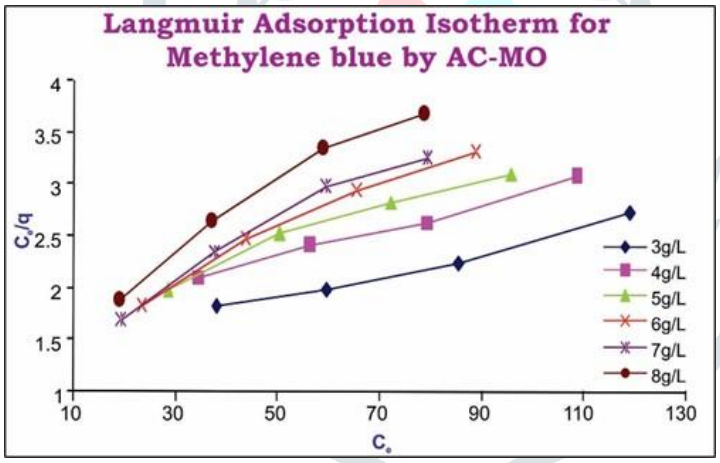

Fig. 10: Langmuir isotherm plot for MB dye adsorption by AC-MO nanoadsorbent.

d. Adsorption kinetic studies

Understanding the dynamics and kinetics of adsorption is essential for comprehending how quickly an adsorbent material captures a solute. The adsorption rate determines how long the solute remains at the interface between the solid adsorbent and the solution. In this study, the researchers analyzed the kinetics of MB (Methylene Blue) adsorption on AC-MO nanoadsorbent using the pseudo-second-order model. This widely-used model describes the adsorption rate as directly proportional to the square of the unadsorbed solute amount and the available adsorption sites on the adsorbent surface. To assess the agreement between experimental data and model-predicted values, the researchers calculated correlation coefficients (R^2 values). A relatively high R^2 value, approaching 1, indicates a strong correlation between the experimental data and the model, demonstrating the effectiveness of the pseudo-second-order model in describing the adsorption kinetics for the AC-MO system. The researchers conducted adsorption kinetics measurements using dye solutions with concentrations of 100, 150, 200, and 250 mg/L at the optimum pH value. These varying concentrations provided comprehensive insights into the adsorption dynamics and how the adsorption rate changes with different initial dye concentrations.

The pseudo-second-order equation is given as follows:

$$\frac{t}{qt} = \frac{1}{h_o} + \frac{1}{(q_e)t} \qquad (7)$$

Where:
h_o is the initial adsorption rate (mg/g min.);
q_e is the amount of dye adsorbed at equilibrium (mg/g);
q_t is the amount of dye adsorbed at time t (mg/g).

The initial adsorption rate, ho, as $t \rightarrow 0$, is defined as:

$ho = K_2 qe^2$

Where:
K_2 is the pseudo-second-order rate constant for the adsorption process (g/mg min.).

The initial adsorption rate, equilibrium adsorption capacity (q_e), and pseudo-second-order rate constant (K_2) were determined from the slope and intercept of the plot of t/qt against t.

By analyzing the adsorption kinetics using the pseudo-second-order model, valuable insights into the rate of adsorption and the behavior of MB dye on the AC-MO nanoadsorbent were obtained. The model's good fit with the experimental data indicates that the adsorption process is well-described by this kinetic model.

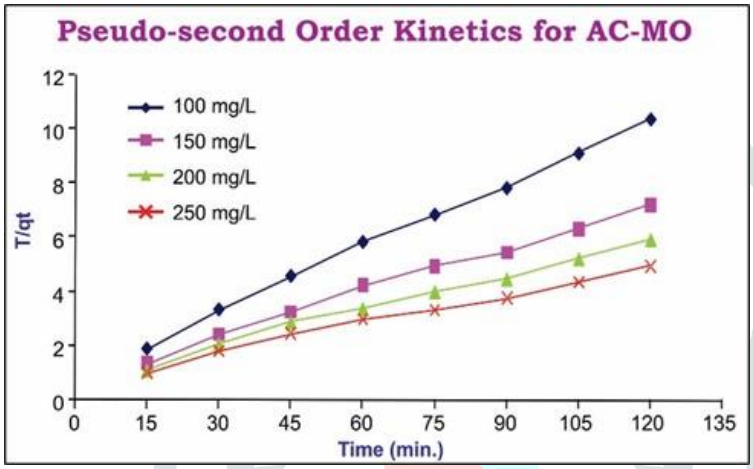

Fig. 11 Pseudo-second order kinetics model for MB dye removal

IV. Conclusion

This study thoroughly investigated the potential of AC-MO nanoadsorbent for adsorbing methylene blue (MB) dye. The findings demonstrated that moringa oleifera seed pod wastes are highly valuable precursors for preparing alternative nanoadsorbents, providing a cost-effective alternative to expensive commercial activated carbon. The study revealed that the optimum pH for MB dye adsorption onto the AC-MO nanoadsorbent was pH 6. Furthermore, the characterization of the nanoadsorbent indicated the presence of large pores, which contributed to its high dye adsorption activity. The adsorption data were well-fitted using the Langmuir Isotherm and pseudo-second-order kinetic model, indicating that the adsorption process followed a monolayer adsorption mechanism and a chemisorption process.

Overall, the study concludes that the nanoadsorbent derived from moringa oleifera seed pod was not only effective in removing MB dye from wastewater but also economically viable, presenting a promising and sustainable solution for water treatment applications. Using waste plant material in preparing the nanoadsorbent highlights the potential for transforming waste into valuable resources for environmental remediation.

V. Acknowledgment

The authors express their sincere gratitude to the following organizations and institutions for their support and contributions to the research:

MRC (Malaviya National Institute of Technology, Jaipur, India)
CAF (Manipal University, Jaipur, India)
Department of Chemistry, University of Rajasthan, Jaipur, India
Department of Physics, University of Rajasthan, Jaipur, India
Indian Institute of Technology, Hyderabad, India

The authors acknowledge these institutions for providing the necessary research facilities and resources that made the study possible. Additionally, they extend special thanks to the University Grants Commission (UGC) of India for their financial assistance, which played a crucial role in supporting the research endeavor

VI. References

[1] Saxena, M.; Sharma, N. and Saxena, R. 2020. Highly efficient and rapid removal of a toxic dye: Adsorption kinetics, isotherm, and mechanism studies on functionalized multiwalled carbon nanotubes. Surfaces and Interfaces, 21(100639). https://doi.org/10.1016/j.surfin.2020.100639

[2] Yaqoob, A. A.; Ahmad, H.; Parveen, T.; Ahmad, A.; Oves, M.; Ismail, I. M.; Qari, H. A.; Umar, K. and Mohamad Ibrahim, M.N. 2020.Recent advances in metal decorated nanomaterials and their various biological applications: A review. Front. Chem., 8: 1-23. https://doi.org/10.3389/fchem.2020.00341

[3] Birniwa, A. H.; Mahmud, H. N. M. E.; Abdullahi, S. S.; Habibu, S.; Jagaba, A. H.; Ibrahim, M. N. M.; Ahmad, A.; Alshammari, M. B.; Parveen, T. and Umar K. 2022. Adsorption Behavior of Methylene Blue Cationic Dye in Aqueous Solution Using Polypyrrole-Polyethylenimine Nano-Adsorbent. Polymers, 14(16): 1-20 https://doi.org/10.3390/polym14163362

[4] Qwane, S.N.; Mdluli, P.S. and Madikizela, L.M. 2020. Synthesis, characterization and application of a molecularly imprinted polymer in selective adsorption of abacavir from polluted water. S. Afr. J. Chem., 73: 84–91. https://doi.org/10.17159/0379-4350/2020/v73a13

[5] Thillainayagam, B. P.; Nagalingam, R. and Saravanan, P. 2023. Batch and column studies on removal of methylene blue dye by microalgae biochar. Biomass Conversion and Biorefnery, 13:10327–10342. https://doi.org/10.1007/s13399-022-03038-3

[6] Chowdhury, S. and Saha, P.D. 2013. Artificial neural network (ANN) modeling of adsorption of methylene blue by NaOH-modified rice husk in a fixed-bed column system. Environ. Sci. Pollut. Res., 20: 1050–1058. https://doi.org/10.1007/s11356-012-0912-2

[7] Yaqoob, A.A.; Ahmad, H.; Parveen, T.; Ahmad, A.; Oves, M.; Ismail, I.M.; Qari, H.A.; Umar, K.; Mohamad Ibrahim, M.N. 2020. Recent advances in metal decorated nanomaterials and their various biological applications: A review. Front. Chem. 8, 341. https://doi.org/10.3389/fchem.2020.00341

[8] Al-Mahbashi, N. M. Y.; Kutty, S. R. M.; Bilad, M. R.; Huda, N.; Kobun, R.; Noor, A.; Jagaba A. H.; Al-Nini, A.; Ghaleb A. A. S. and Saleh Al-dhawi, B. N. 2022. Bench-Scale Fixed-Bed Column Study for the Removal of Dye-Contaminated Effluent Using Sewage-Sludge-Based Biochar. Sustainability, 14: 6484 https://doi.org/10.3390/su14116484

[9] Choi, Y.K.; Choi, T.R.; Gurav, R.; Bhatia, S.K.; Park, Y.L.; Kim, H.J.; Kan, E. and Yang, Y.H. 2020. Adsorption behavior of tetracycline onto Spirulina sp. (microalgae)-derived biochars produced at different temperatures. Sci. Total Environ., 710: 136282. https://doi.org/10.1016/j.chemosphere.2020.128539

[10] Shi, Q.; Wang, W.; Zhang, H.; Bai, H.; Liu, K.; Zhang, J.; Li, Z.; Zhu, W. 2023. Porous biochar derived from walnut shell as an efficient adsorbent for tetracycline removal. Bioresource Technology, 383: 129213 https://doi.org/10.1016/j.biortech.2023.129213

[11] Oyekanmi, A. A.; Latiff, A. A. A.; Daud, Z.; Mohamed, R.; Aziz, N.; Ismail, N.; Rafatullah, M.; Ahmad, A.; Hossain, K. 2019. Adsorption of pollutants from palm oil mill effluent using natural adsorbents: Optimization and isotherm studies. Desalin. Water Treat., 169: 181–190. http://doi.org/10.5004/dwt.2019.24689

[12] Al-Gheethi, A. A.; Azhar, Q. M.; Kumar, P. S.; Yusuf, A. A.; Al-Buriahi, A. K.; Mohamed S. M. S. R.; Al-shaibani, M. M. 2022. Sustainable approaches for removing Rhodamine B dye using agricultural waste adsorbents: A review. Chemosphere, 287(2): 132080. https://doi.org/10.1016/j.chemosphere.2021.132080

[13] Alhogbi, B. G.; Altayeb, S.; Bahaidarah, E. A. and Zawrah, M. F. 2021. Removal of Anionic and Cationic Dyes from Wastewater Using Activated Carbon from Palm Tree Fiber Waste. Processes, 9: 416 https://doi.org/10.3390/pr9030416

[14] Suhas; Gupta, V. K.; Carrott, P. J. M.; Singh, R.; Chaudhary, M.; Kushwaha, S. 2016. Cellulose: A review as natural, modified and activated carbon adsorbent. Bioresour. Technol., 216:1066–1076. https://doi.org/10.1016/j.biortech.2016.05.106.

[15] Silva, T.L.; Cazetta, A.L.; Souza, P.S.C.; Zhang, T.; Asefa, T.; Almeida, V.C. 2018. Mesoporous activated carbon fibers synthesized from denim fabric waste: Efficient adsorbents for removal of textile dye from aqueous solutions. J. Clean. Prod.,171: 482–490. https://doi.org/10.1016/j.jclepro.2017.10.034

[16] Beltrán- Heredia, J.; Sánchez-Martín, J. and Delgado-Regalado, A. 2009. Removal of Dyes by Moringa oleifera Seed Extract. Study through Response Surface Methodology. Journal of Chemical Technology & Biotechnology, 84: 1653–1659. https://doi.org/10.1002/jctb.2225

[17] Azad, M. S. and Hassan, M.S. 2020. Importance of Moringa Oleifera for Wastewater Treatment: A Review. International Journal of Sustainable Energy Development, 8 (1): 415-420. https://doi.org/10.20533/ijsed.2046.3707.2020.0049

[18] Desta, W. M. and Bote, M. E. 2021. Wastewater treatment using a natural coagulant (Moringa oleifera seeds): optimization through response surface methodology. Heliyon. 7:e08451 https://doi.org/10.1016/j.heliyon.2021.e08451

[19] Thanki, A.; Padhiyar, H.; Kathiriya, T. and Shah, D. 2020. Applications of Moringa Oleifera for Wastewater Treatment: Concepts and Approaches. Green Innovation, Sustainable Development, and Circular Economy, 1:9. https://doi.org/10.1201/9781003011255-11

[20] Siong, V. L. E.; Lee, K. M.; Juan, J. C.; Lai, C. W.; Tai, X. H. and Khe, C.S. 2019. Removal of methylene blue dye by solvothermal reduced graphene oxide: a metal-free adsorption and photodegradation method. RSC Advances, 9: 37686-37695. https://doi.org/10.1039/c9ra05793e

[21] Hassaan M. A.; Yılmaz M.; Helal, M.; El-Nemr, M. A.; Ragab, S. and Nemr, A.E. 2023. Improved methylene blue adsorption from an aqueous medium by ozone-triethylenetetramine modification of sawdust-based biochar. scientific reports, 13:12431 https://doi.org/10.1038/s41598-023-39495-7

[22] Shah, S. S.; Sharma, T.; Dar, B. A. and Bamezai, R. K. 2021. Adsorptive removal of methyl orange dye from aqueous solution using populous leaves: Insights from kinetics, thermodynamics and computational studies. Environmental Chemistry and Ecotoxicology, 3:172-181 https://doi.org/10.1016/j.enceco.2021.05.002

[23] Vinayagam, R.; Pai, S.; Murugesan, G.; Varadavenkatesan, T.; Kaviyarasu K. and Selvaraj, R. 2022 Green synthesized hydroxyapatite nanoadsorbent for the adsorptive removal of AB113 dye for environmental applications. Environmental Research, 212 B: 113274. https://doi.org/10.1016/j.envres.2022.113274

[24] Nwosu, F. O.; Ajala, O. J.; Owoyemi, R. M. and Raheem, B. G. 2018. Preparation and characterization of adsorbents derived from bentonite and kaolin clays. Applied Water Science, 8:195. https://doi.org/10.1007/s13201-018-0827-2

[25] Moustafa, M. T. 2023. Preparation and characterization of low-cost adsorbents for the efficient removal of malachite green using response surface modeling and reusability studies. Scientific Reports, 13:4493. https://doi.org/10.1038/s41598-023-31391-4

[26] Meena, P. L.; Saini, J. K.; Surela, A. K.; Mordhiya, B.; Chhachhia, L. K.; Meena K.S. 2022. Fabrication of Polyaniline-Supported MnO_2 Nanocomposite for Removal of Water Pollutant: Kinetic and Isotherm Studies. Biomass Conversion and Biorefinery, https://doi.org/10.1007/s13399-021-02267-2

[27] Mohammed, A. J.; Ibrahim, M. H.; Zulkifli, S. Z. Salman J. M. 2021. Synthesis and Characterization of a Nano-Adsorbent Derivative Derived from Grape Seeds for Cadmium Ion Removal in an Aqueous Solution. Water, 13(20): 2896 http://dx.doi.org/10.3390/w13202896

[28] Kaliannan, D.; Palaninaicker, S.; Palanivel, V.; Mahadeo, M. A.; Bulakhe N. Ravindra & Shim Jae-Jin A novel approach to preparation of nano-adsorbent from agricultural wastes (Saccharum officinarum leaves) and its environmental application, https://doi.org/10.1007/s11356-018-3734-z

[29] Dryaz, A. R.; Shaban, M.; AlMohamadi, H.; Abu Al-Ola, K. A.; Hamd, A.; Soliman, N. K. and Ahmed, S. A. 2021. Design, characterization, and adsorption properties of Padina gymnospora/zeolite nanocomposite for Congo red dye removal from wastewater. Environmental Science and Pollution Research, 11:21058. https://doi.org/10.1038/s41598-021-00025-y

[30] Vanlalveni, C.; Lallianrawna, S.; Biswas, A.; Selvaraj, M.; Changmai, B. and Rokhum S. L. 2021. Green synthesis of silver nanoparticles using plant extracts and their antimicrobial activities: a review of recent literature. RSC Adv., 11(5): 2804-2837. https://doi.org/ 10.1039/d0ra09941d.

[31] Kaur, C.; Roy, T.; Das, S.; Gupta, R. and Pramanik T. 2023. Preparation and application of bio-adsorbent for the removal of water hardness: conversion of a waste to a value-added material. Biomass Conversion and Biorefinery, 13: 8161-8171. https://doi.org/10.1007/s13399-021-01806-1

[32] Harsha, K. R. S.; Murthy, M.; Udayasimha, L.; Dharmaprakash and Rangappa, D. 2017. Synthesis and Characterization of Activated Carbon Coated Alumina as Nano Adsorbent. 4 (11): 12321-12327 https://doi.org/10.1016/j.matpr.2017.09.166

[33] El-Nemr, M. A.; Yılmaz, M.; Ragab, S.; Hassaan, M. A. and El Nemr,A. 2023. Isotherm and kinetic studies of acid yellow 11 dye adsorption from wastewater using Pisum Sativum peels microporous activated carbon, Scientific report, 13:4268. https://doi.org/10.1038/s41598-023-31433-x

[34] Nnadozie, E. C. and Ajibade, P. A. 2021. Isotherm, kinetics, thermodynamics studies and effects of carbonization temperature on adsorption of Indigo Carmine (IC) dye using C. odorata biochar. Chemical Data Collections. 33: 100673. https://doi.org/10.1016/j.cdc.2021.100673

[35] Wong, S.; Ghafar, N. A.; Ngadi, N.; Razmi, F. A.; Inuwa, I. M.; Mat, R. and Amin, N. A. S. 2020. Effective removal of anionic textile dyes using adsorbent synthesized from coffee waste. Scientific Reports, 10:2928, https://doi.org/10.1038/s41598-020-60021-6